厚生労働科学研究費補助金

障害者対策総合研究事業

動脈ラベル標識法（ASL）を用いた精神疾患の脳画像解析法の確立

平成24年度　総括研究報告書

研究代表者　太田深秀

平成 25（2013）年　4 月

目　　次

厚生労働科学研究費補助金（障害者対策総合研究事業）
総括研究報告書

動脈ラベル標識法（ASL）を用いた精神疾患の脳画像解析法の確立に関する研究

研究代表者　太田　深秀　国立精神・神経医療研究センター神経研究所
疾病研究第三部　室長

研究要旨

近年3テスラのMRIの普及に伴いASLによる局所脳血流量測定が注目されている。そこで我々はうつ病や統合失調症などを対象とした精神疾患の脳データーバンクの作成を行い、脳形態画像とASLとを組み合わせた新しい精神疾患の客観的診断法を確立することを目的とする。

太田　深秀
国立精神・神経医療研究センター神経研究所疾病研究第三部　室長

A．研究目的

近年の研究により、統合失調症における局所脳変化が明らかとなってきている。また形態学的変化のみならず、これまで SPECT や PET を用いた脳血流検査を対象とした疾患研究でも統合失調症患者における特異な変化が認められている。しかしながら、現状では疾患診断は医師の診察によってのみ行われており、重症度の判定や予測も現症などからのみ判断されてきた。このたび我々は multimodal neuroimaging を用いて統合失調症における変化について注目した。

B．研究方法

当センターで統合失調症と診断を受けた方 36 人と年齢、性別を適合させた健常被験者 42 人を対象に 3T の MRI スキャナにより 3D-T1weighted image と DTI、pCASL による ASL を撮影し、健常群と疾患群における差異を検証した。また、今回の ASL の検証には BPM を用い各ボクセルの皮質容量を共変量に入れることで、局所容積効果による影響を除外した。

（倫理面への配慮）

対象者には検査に関する説明を行い、文書にて同意を得た。

C．研究結果

統合失調症患者群では左下前頭前野の皮質容量、上側頭領域～左外包～左前頭前野領域のFA値の低下を認めた。さらに統合失調症患者では左前頭前野などにおける脳血流低下を確認しており、前述の大脳皮質容量を対象とした検証、白質病変を対象とした検証で認められた障害部位と合致した。この結果はこれまでの先行研究で統合失調症における変化が確認されている領域と一致した。

D．考察

ASLは解像度が決して高くなく、ノイズの流入により平均値の異常上昇がみられていた。しかしmedian filterによる処置にて良好なデータを得ることが可能となった。

E.結論

統合失調症では陽性症状の消長と関連して脳血流に増減があることがしばしば指摘されていることから、左下前頭前野の血流低下はtraitとして指標に利用できる可能性が示唆された。

F．健康危険情報

特記事項なし

G．研究発表

1．　論文発表

Ota M et al: Magnetic Resonance Imaging　in press.

Ota M et al: Brain Research 1499:61-68, 2013.

2．　学会発表

現在投稿準備中

H．知的財産権の出願・登録状況

1．特許取得
予定なし

2．実用新案登録
予定なし

3．その他
特記事項なし

研究成果の刊行に関する一覧表レイアウト

雑誌

発表者氏名	論文タイトル名	発表誌名	巻号	ページ	出版年
Miho Ota et al	Abnormalities of cerebral blood flow in multiple sclerosis: A pseudocontinuous arterial spin labeling MRI study	Magnetic Resonance Imaging	In press		2013
Miho Ota et al	Multimodal image analysis of sensorimotor gating in healthy women.	Brain Research	1499	61-68	2013

書籍

著者氏名	論文タイトル名	書籍全体の編集者名	書　籍　名	出版社名	出版地	出版年	ページ
該当なし							

BRAIN RESEARCH 1499 (2013) 61–68

Available online at www.sciencedirect.com

SciVerse ScienceDirect

www.elsevier.com/locate/brainres

Brain Research

Research Report

Multimodal image analysis of sensorimotor gating in healthy women

Miho Ota[a,*], *Noriko Sato*[b], *Junko Matsuo*[a], *Yukiko Kinoshita*[a], *Yumiko Kawamoto*[a], *Hiroaki Hori*[a], *Toshiya Teraishi*[a], *Daimei Sasayama*[a], *Kotaro Hattori*[a], *Satoko Obu*[a], *Yasuhiro Nakata*[b], *Hiroshi Kunugi*[a]

[a]*Department of Mental Disorder Research, National Institute of Neuroscience, National Center of Neurology and Psychiatry, 4-1-1 Ogawa-Higashi, Kodaira, Tokyo 187–8502, Japan*

[b]*Department of Radiology, National Center of Neurology and Psychiatry, 4-1-1 Ogawa-Higashi, Kodaira, Tokyo 187-8551, Japan*

ARTICLE INFO

Article history:
Accepted 29 December 2012
Available online 16 January 2013

Keywords:
Diffeomorphic anatomical registration using exponentiated lie algebra
Diffusion tensor imaging
Prepulse inhibition
Tract-based spatial statistics

ABSTRACT

Prepulse inhibition (PPI) deficits have been reported in individuals with schizophrenia and other psychiatric disorders with dysfunction of the cortico–striato–pallido–thalamic circuit. The purpose of this study was to investigate the structural neural correlates of PPI by using magnetic resonance imaging (MRI) metrics. The subjects were 53 healthy women (mean age; 40.7 ± 11.3 years). We examined the possible relationships between PPI and diffusion tensor imaging (DTI) metrics to estimate white matter integrity and gray matter volume analyzed using the DARTEL (diffeomorphic anatomical registration through exponentiated lie) algebra method. There were significant correlations between DTI metrics and PPI in the parahippocampal region, the anterior limb of the internal capsule, the ventral tegmental area, the thalamus and anterior thalamic radiations, the left prefrontal region, the callosal commissural fiber, and various white matter regions. There were also positive correlations between PPI and gray matter volume in the bilateral parietal gyri and the left inferior prefrontal gyrus at a trend level. The present study revealed evidence of a relationship between PPI and the integrity of white matter. This result was compatible with the previous suggestion that PPI would be modulated by the cortico-striato-thalamic-pallido-pontine circuit.

Abbreviations: 3-dimensional (3D), blood oxygenation level-dependent (BOLD); cerebrospinal fluid (CSF), diffeomorphic anatomical registration using exponentiated lie algebra (DARTEL); diffusion tensor imaging (DTI), echo time (TE); false discovery rate (FDR), family-wise error (FWE); field of view (FOV), fluid attenuation inversion recovery (FLAIR); fractional anisotropy (FA), functional magnetic resonance imaging (fMRI); mean diffusivity (MD), Mini-International Neuropsychiatric Interview (MINI); positron emission tomography (PET), prepulse inhibition (PPI); repetition time (TR), statistical parametric mapping (SPM); threshold-free cluster enhancement (TFCE), tract-based spatial statistics (TBSS). voxel-based morphometry (VBM).

*Corresponding author. Fax: +81 42 346 2094.
E-mail address: ota@ncnp.go.jp (M. Ota).

0006-8993/$ - see front matter © 2013 Elsevier B.V. All rights reserved.
http://dx.doi.org/10.1016/j.brainres.2012.12.044

1. Introduction

The startle reflex can be attenuated when the startling stimulus is preceded by a weak non-startling prepulse, in a process called prepulse inhibition (PPI). The degree to which such a prepulse inhibits the startle reflex in PPI is used as a measure of sensorimotor gating. Disruptions in information processing and attention have long been thought of as one of the hallmarks of schizophrenia (McGhie and Chapman, 1961), and PPI has been suggested as a neurophysiologic measure of information processing abnormalities in schizophrenia (Cadenhead and Braff, 1999).

There is evidence from animal studies that PPI is modulated by forebrain circuits involving the prefrontal cortex, thalamus, hippocampus, amygdala, nucleus accumbens, striatum, and globus pallidus (Koch and Schnitzler, 1997; Swerdlow and Geyer, 1998; Swerdlow et al., 2001). Deficient PPI is observed in several neuropsychiatric disorders characterised by abnormalities in the cortico-striato-thalamic-pontine circuitry (Braff et al., 2001; Swerdlow et al., 2008). Previous neuroimaging studies using structural brain images revealed the neural correlates of PPI in the prefrontal and orbitofrontal cortex, hippocampus extending to the parahippocampal gyrus, the basal ganglia including parts of putamen, the globus pallidus, and the nucleus accumbens, posterior cingulate, superior temporal gyrus, and thalamus (Kumari et al., 2005, 2008a). Several functional magnetic resonance imaging (fMRI) studies showed that PPI is associated with increased bilateral activation in the striatum extending to the hippocampus, insula, thalamus, and inferior frontal, middle temporal, and inferior parietal lobes (Hazlett et al., 2001, 2008; Kumari et al., 2003, 2008a). A regression analysis demonstrated a linear relationship between PPI and blood oxygenation level-dependent (BOLD) activity in the thalamus, nucleus accumbens, and inferior parietal region (Kumari et al., 2003). Positron emission tomography (PET) study also detected an association between PPI and the prefrontal and inferior parietal cortices' glucose metabolism (Hazlett et al., 1998). Although it is known that PPI disruption resulted from the interruption of the cortico–striato–thalamic–pontine neural circuit, to our knowledge there has been no study verifying the integrity of white matter using diffusion tensor imaging (DTI).

The present study was conducted to investigate the structural basis of PPI deficits using DTI and volumetry analysis. We hypothesized that PPI would be correlated with components in the hippocampus/temporal lobe, basal ganglia, cingulate gyrus, and frontal and parietal regions.

2. Results

Initially, we examined the correlation between the gray matter volume and % PPI using DARTEL (diffeomorphic anatomical registration using exponentiated lie). There was no significant correlation between them; however, there were nominal trends between % PPI with 90 dB prepulse and gray matter volume in the bilateral parietal gyri and left inferior prefrontal regions ($p<0.005$ uncorrected) (Fig. 1(A)), and between % PPI with 86 dB prepulse and gray matter volume in the left parietal and medial frontal regions ($p<0.005$ uncorrected) (Fig. 1(B)).

We then examined correlation between % PPI and DTI. Significant positive correlations were observed between fractional anisotropy (FA) value and % PPI with 90 dB prepulse in the right ventral tegmental area, left anterior limbs of the internal capsule, bilateral thalami, and the left inferior prefrontal region, bilateral medial frontal regions, and bilateral parietal regions ($p<0.001$ uncorrected) (Fig. 2(A) to (F)), however, we could detect correlation between % PPI with 86 dB prepulse and FA values only in the inferior prefrontal region (Fig. 2(G)) ($p<0.001$ uncorrected). In addition, analysis using the skeletonized FA data showed that there were significant positive correlations between FA value and % PPI with 90 dB prepulse in the parahippocampal region, orbitofrontal region, bilateral temporal–inferior parietal regions, internal capsule,

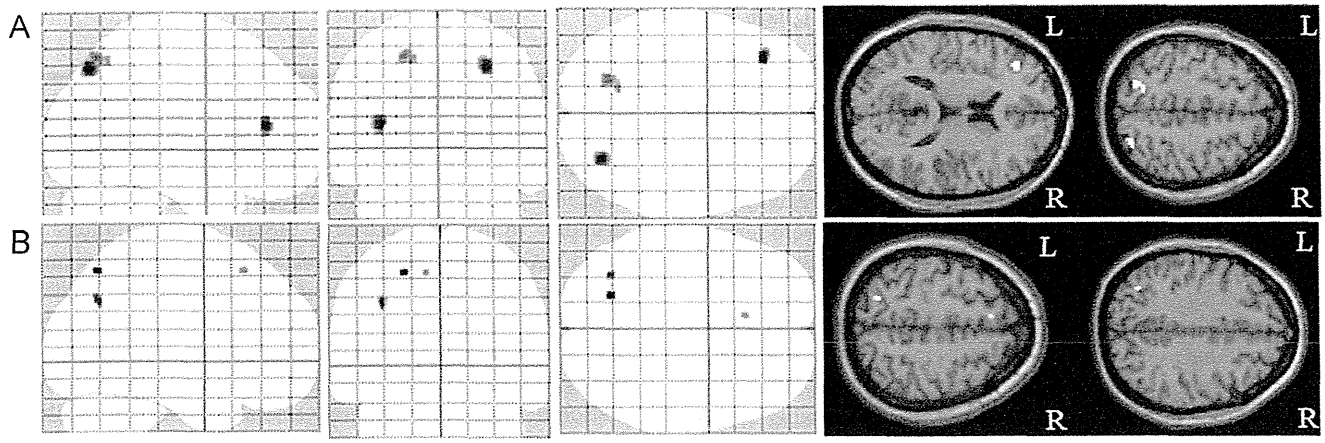

Fig. 1 – Brain areas in which % PPI and gray matter volume showed correlation. There was no significant correlation between % PPI and gray matter volume. However, a nominal trend was found in the bilateral parietal regions and left inferior prefrontal regions (A) ($p<0.005$ uncorrected). Likewise, there was a nominal correlation between % PPI with 86 dB prepulse and gray matter volume in the left parietal and medial frontal regions (B) ($p<0.005$ uncorrected). Age and whole brain volume were controlled. L, left; R, right.

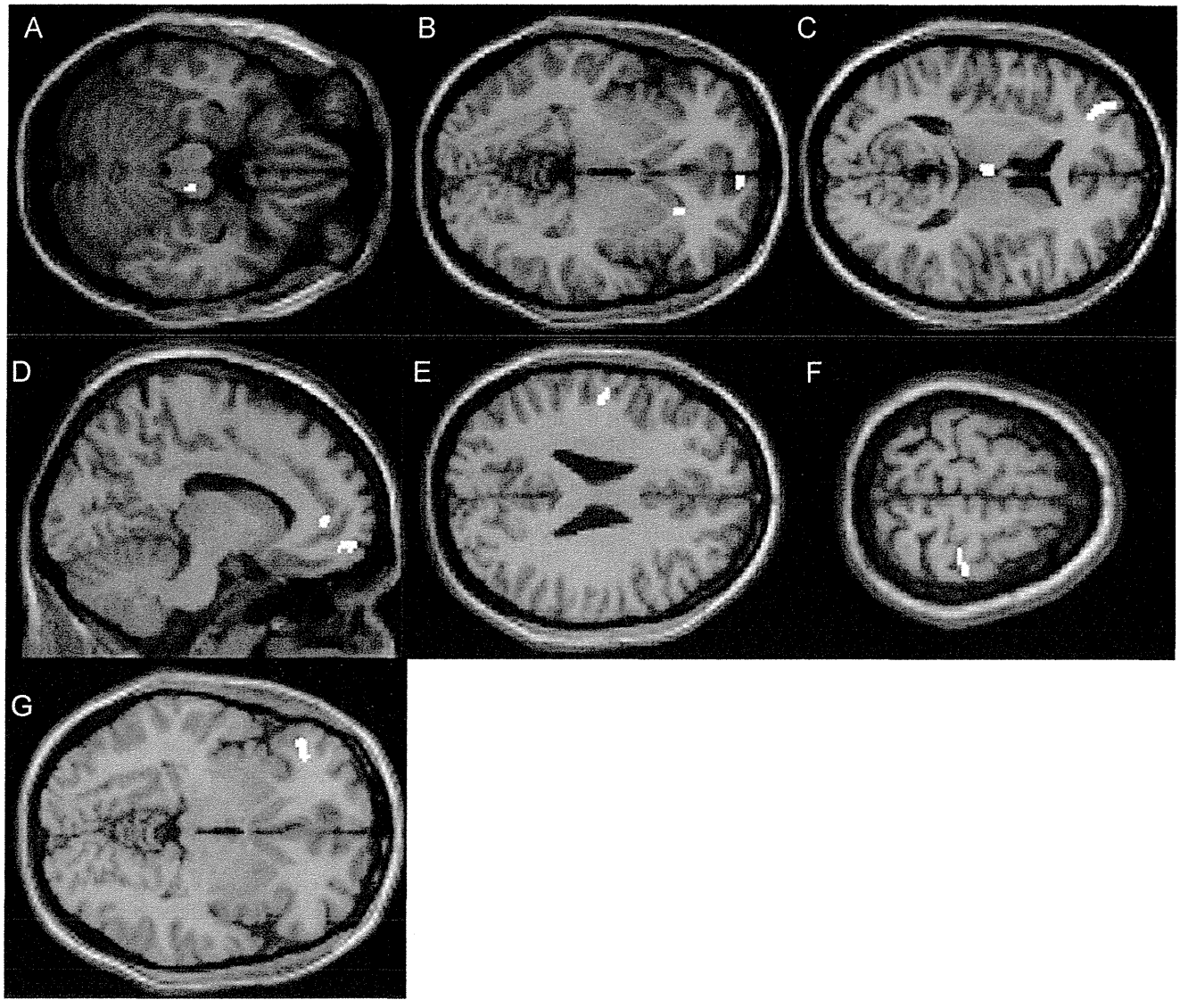

Fig. 2 – Brain areas in which % PPI and FA values correlated. There were positive correlations between % PPI with 90 dB of prepulse and FA values in the right ventral tegmental area (A), left anterior limbs of internal capsule (B), bilateral thalami, and left inferior prefrontal region (C), bilateral medial frontal regions ((B), (D)), and bilateral parietal regions ((E) and (F)) ($p<0.001$ uncorrected). Correlation between % PPI with 86 dB of prepulse and FA values was seen only in the inferior prefrontal region (G) ($p<0.001$ uncorrected). Age was controlled. L, left; R, right.

thalamus, anterior thalamic radiations, posterior cingulate, and callosal commissural fibers ($p<0.05$, family-wise error (FWE) rate is controlled) (Fig. 3(A) to (D)). On the other hand, there were no significant correlation between % PPI with 86 dB prepulse and FA value, and only nominal trends were revealed in similar regions (Fig. 3(E) to (H)) ($p<0.1$; FWE rate is controlled).

There were significantly positive correlations between % PPI and the mean diffusivity (MD) values in many regions throughout the brain (90 dB; Fig. 4(A), 86 dB; Fig. 4(B)). To be more conservative, we corrected for multiple testing by false discovery rate (FDR) and set the critical p-value as <0.01(90 dB), and by FWE and set the critical p-value as <0.05 (86 dB). After this procedure, the correlations of PPI with MD values in the left inferior prefrontal region remained significant (Fig. 4(A) and (B), the right column).

3. Discussion

To our knowledge, this is the first study that used DTI to examine the possible relationships between PPI and brain structure in healthy subjects. Significant correlations were noted between PPI and DTI metrics in the ventral tegmental area, parahippocampus, callosal commissural fiber, thalamus, anterior thalamic radiation, internal capsule, posterior cingulate, and temporal and parietal regions. There were nominal trends between PPI and gray matter volume in the left inferior prefrontal region and bilateral parietal regions. Our results are consistent with previous neuroimaging studies using structural MRI and fMRI and pharmacological studies (Hazlett et al., 2001; Kumari et al., 2005; Swerdlow et al., 2001).

Consistent with the consensus regarding PPI in the rat, a number of psychiatric and neurological disorders characterized

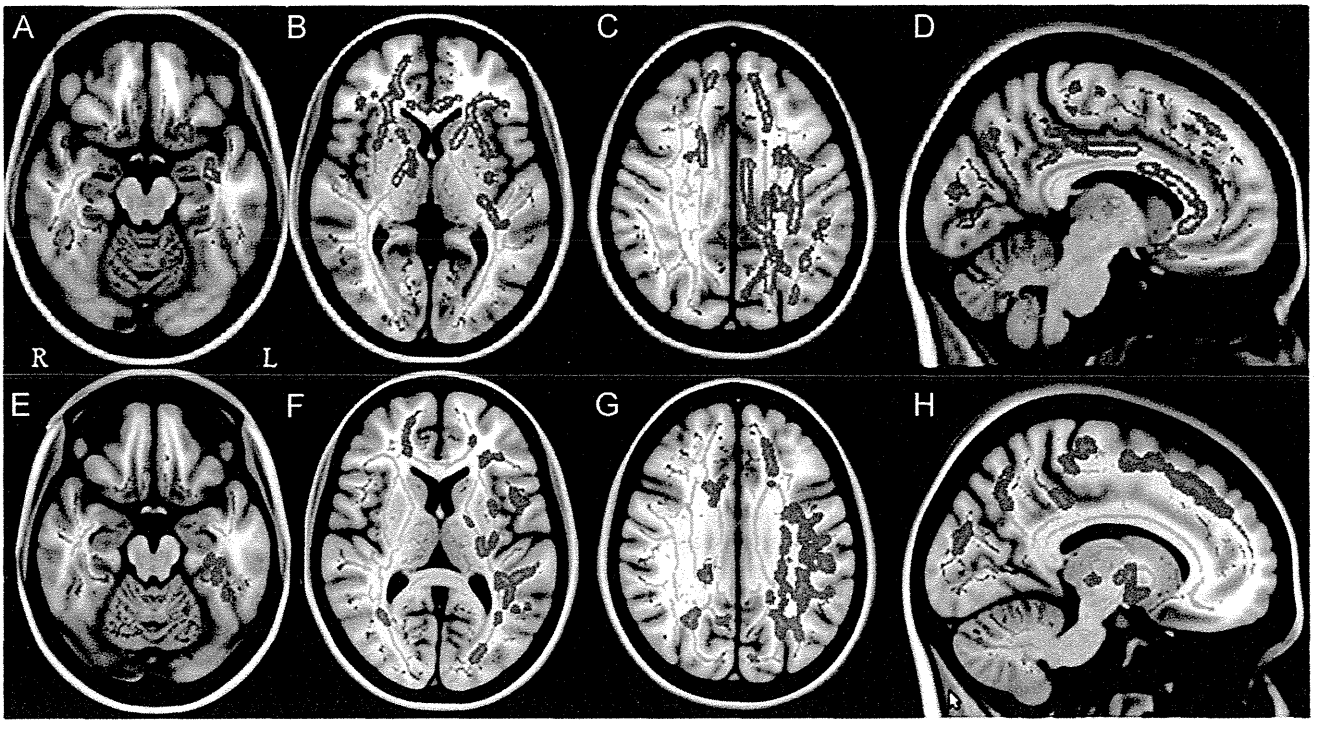

Fig. 3 – Brain areas in which % PPI and FA values correlated using TBSS. There were positive correlations between % PPI with 90 dB of prepulse and FA values in the parahippocampal region (A), orbitofrontal region (A), temporal–parietal regions ((B) and (C)), internal capsules (B), thalamus and anterior thalamic radiations ((B) and (C)), posterior cingulate ((C) and (D)), and anterior dominant callosal commissural fibers ((B) and (D)) revealed by tract-based spatial statistics (TBSS) ($p<0.05$; family-wise error rate is controlled). On the other hand, there were no significant correlations between % PPI with 86 dB of prepulse and FA values, however, a nominal trend was detected in similar regions ((E) to (H)) ($p<0.1$; family-wise error rate is controlled). Age was controlled. The skeleton, shown in green, is thresholded at 0.2 and overlaid onto the MNI152 space. L, left; R, right. (For interpretation of the references to colour in this figure legend, the reader is referred to the web version of this article.)

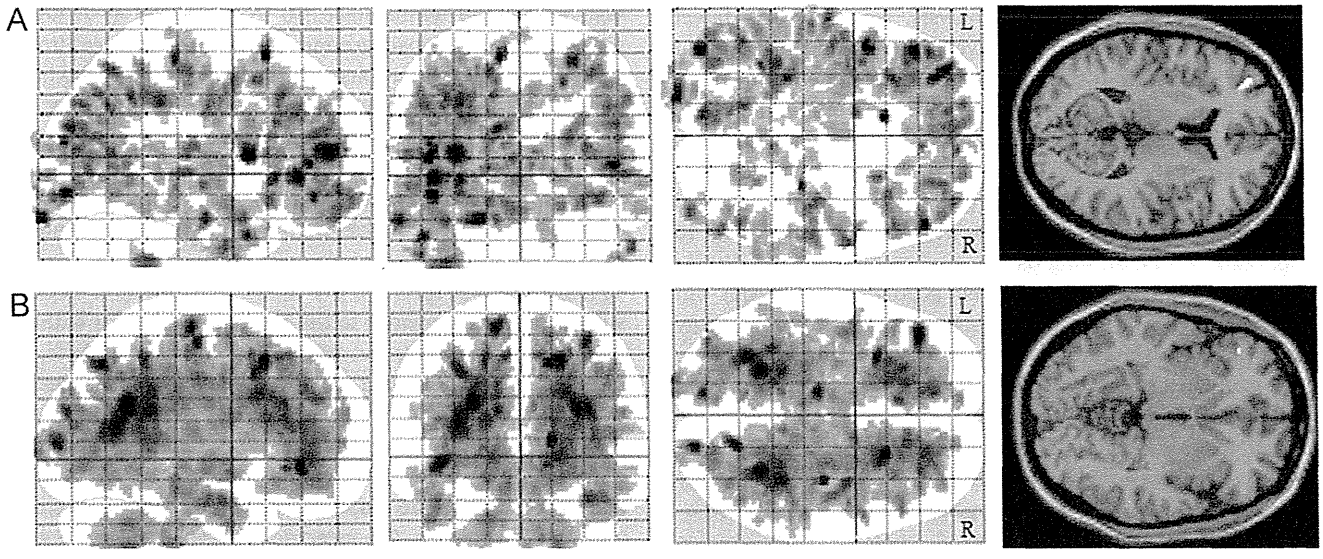

Fig. 4 – Brain areas in which % PPI and MD values correlated. There were negative correlations between % PPI with 90 (A) and 86 dB (B) of prepulse and MD values in several areas throughout the brain ($p<0.001$ uncorrected). The right column showed that the correlations remained when we re-analyzed the correlation between PPI and MD values in the left inferior prefrontal region (90 dB; $p<0.01$ [false discovery rate], 86 dB; $p<0.05$ [family-wise error rate]). L, left; R, right.

by abnormalities at some level in the cortico–striato–thalamic–pontine circuitry (Braff et al., 2001; Swerdlow et al., 2008) and in the cortico–striato–pallido–thalamic brain substrate (Perry et al., 2004; Swerdlow et al., 2008) showed the PPI deficient. Previous neuroimaging studies revealed the correlation between PPI and regional brain using structural brain images (Kumari et al., 2005,

2008b), and fMRI (Hazlett et al., 2001, 2008; Kumari et al., 2003, 2007, 2008a). Here we found significant correlations between PPI and DTI metrics in the parahippocampus, the internal capsule, the circumference of anterior thalamic radiation and the parietal region. In light of these observations, PPI may be regulated through an amygdala – basal ganglia – prefrontal and parietal circuit. There is evidence from animal studies that PPI is mediated by brain stem circuits involving the inferior colliculus, superior colliculus, pedunculopontine tegmental nucleus, laterodorsal tegmental nucleus, substantia nigra pars reticulata, and caudal pontine reticular nucleus (Fendt et al., 2001). In the present study, we detected a correlation between FA in the ventral tegmental area and % PPI, a finding that is compatible with this previous evidence.

As described above, previous studies showed that PPI is influenced by many regions throughout the brain, and PPI is thought to be affected by the transmission of information. We therefore hypothesized that to evaluate the relation between PPI and the brain, the use of DTI – which shows the condition of the neural fibers – would be effective. Our DTI results suggested that a large area of the brain is involved in deficits in PPI, compared to the foregoing studies focusing on the gray matter. This may be due to the ability of DTI to delineate neural pathways. Furthermore, we detected more correlations between % PPI and brain metrics when prepulse was 90 dB than when it was 86 dB. Previous studies showed that % PPI at the prepulse intensity of 90 dB was higher compared with that at 86 dB, and that the difference in % PPI between patients with schizophrenia and healthy controls became most significant when prepulse was 90 dB (Kunugi et al., 2007; Takahashi et al., 2008; Moriwaki et al., 2009). These points may suggest that % PPI with 90 dB of prepulse is the best condition to reflect his/her own information processing and attention.

Regarding the volumetric analysis, we could not detect any significant relationship between the PPI and gray matter volume, although the data showed a nominal trend of a relationship in the inferior frontal gyrus and bilateral parietal regions. As to the association between the inferior prefrontal region and PPI, we detected this relationship by all metrics used in this study. This connection was previously detected in an MRI volumetric study (Kumari et al., 2005). However, 10 men and 14 women took part in that study. Previous studies showed a gender difference in PPI (Kumari. et al., 2004), but we evaluated only female subjects. We failed to detect any significant correlation between PPI and gray matter volume. The inconsistent results between previous studies and ours may be attributable, at least in part, to the fact that we examined only females who showed a narrow range of PPI. In conjunction with this, our study included only healthy women whose % PPI was changeable along with the menstrual cycle status (Swerdlow et al., 1997). Further studies work with information on menstrual cycle and studies on male subjects are necessary to address this issue.

In conclusion, the present study examined structural neural correlates of PPI and revealed evidence of a relationship between PPI and the integrity of white matter in healthy women. These observations confirm the involvement of these regions in human PPI as suggested by previous relevant data. Further research should extend the present methods in studies of clinical populations.

4. Experimental procedures

4.1. Sample

The subjects were 63 healthy females who were recruited from the community through local magazine advertisements and our website announcement. The participants were interviewed for enrollment using the Japanese version of the Mini-International Neuropsychiatric Interview (MINI) (Otsubo et al., 2005; Sheehan et al., 1998) by research psychiatrists, and only those who demonstrated no history of psychiatric illness or contact with psychiatric services were enrolled in the study. Participants were excluded if they had a prior medical history of central nervous system disease or severe head injury. In addition, 10 non-responders to the startle stimulus (see the "*Prepulse inhibition measure*" below) were also excluded from the analysis. As a consequence, 53 healthy females (mean age; 40.7±11.3 years, education; 14.8±2.7 years) took part in the study.

Written informed consent was obtained for participation in the study from all subjects, and the study was approved by the Ethics Committee of the National Center of Neurology and Psychiatry, Tokyo, Japan.

4.2. Prepulse inhibition measure

Our equipment, setup, and standard PPI testing procedures have been described in detail (Kunugi et al., 2007). The startle reflex to acoustic stimuli was measured using the Startle Reflex Test Unit for Humans (O'Hara Medical, Tokyo). Subjects refrained from smoking for at least 20 min prior to the test. Broadband white noise (50 to 24,000 Hz) at 70 dB was presented as the background noise and was continuous throughout the session. Acoustic startle stimuli of the broadband white noise were presented through headphones.

During the initial 3 min of each session, the background noise alone was given for acclimation. In total, 35 startle-response trials were recorded in a session. These trials consisted of three blocks. In the first block, the subject's startle response to a pulse (sound pressure: 115 dB; duration: 40 ms) alone was recorded five times. In the second block, the subject's startle response to the same pulse with or without a prepulse (sound pressure: 86 or 90 dB; duration: 20 ms; lead interval [onset to onset]: 60 or 120 ms) was measured five times for each condition. The differential conditions of trials were presented in a pseudo-random order; however, the order was the same for all of the subjects. In the third and final block, the startle response to the pulse alone was again measured five times. The intertrial intervals (15 s on average, range 10 to 20 s) were randomly changed. The entire session lasted approximately 15 min. The mean % PPI of startle magnitude was calculated using the following formula, because in a previous study this condition showed the best sensitivity to differentiate between schizophrenic patients and healthy subjects (Kunugi et al., 2007):

% PPI = 100 × (magnitude on pulse-alone trials − magnitude on prepulse trials {sound pressure: 86 dB and 90 dB; lead

interval: 120 ms, right eye])/magnitude on pulse-alone trials in the 2nd block.

The mean % PPI of the 53 subjects were 45.9±54.7 under the terms of 86 dB, and 58.8±39.8 of 90 dB. We defined *a priori* the "non-responders" to the startle stimuli as those subjects for whom the average value of the startle magnitude in the pulse-alone trials was <0.05 (digital unit), and the non-responders were excluded from the analysis.

4.3. MRI data acquisition

4.3.1. Data acquisition

MR imaging was performed on a Magnetom Symphony 1.5-T system (Siemens, Erlangen, Germany). High spatial resolution, 3-dimensional (3D) T1-weighted images of the brain were obtained for the morphometric study. The 3D T1-weighted images were scanned in the sagittal plane (echo time (TE)/repetition time (TR): 2.64/1580 ms; flip angle: 15°; effective slice thickness: 1.23 mm; slab thickness: 177 mm; matrix: 208 × 256; field of view (FOV): 256 × 315 mm^2; acquisition: (1), yielding 144 contiguous slices through the head.

DTI was performed in the axial plane (TE/TR: 106/11,200 ms; FOV: 240 × 240 mm^2; matrix: 96 × 96; 75 continuous transverse slices; slice thickness 2.5 mm with no interslice gap; acquisitions: (2). Diffusion was measured along 12 non-collinear directions with the use of a diffusion-weighted factor, *b*, in each direction for 1000 s/mm^2, and one image was acquired without use of a diffusion gradient. The DTI examination took approx. 6 min. In addition to DTI and 3D T1-weighted images, conventional axial T2-weighted images (TE/TR: 95/3500 ms; flip angle: 150°; slice thickness: 5 mm; intersection gap: 1.75 mm; matrix: 448 × 512; FOV: 210 × 240 mm^2; acquisitions: (1), and fluid attenuation inversion recovery (FLAIR) images in the axial plane (TE/TR: 101/8800 ms; flip angle: 150°; slice thickness: 3 mm; intersection gap: 1.75 mm; matrix: 448 × 512; FOV: 210 × 240 mm^2; acquisition: (1) were acquired to exclude cerebrovascular disease. On conventional MRI, no abnormal findings were detected in the brain in any subject.

4.3.2. Diffeomorphic anatomical registration using exponentiated lie analysis

The raw 3D T1-weighted volume data were transferred to a workstation. A preprocessing step of voxel-based morphometry (VBM) in Statistical Parametric Mapping (SPM) was improved with the DARTEL registration method (Ashburner, 2007). This technique, being more deformable, notably improves the realignment of small inner structures (Yassa and Stark, 2009). Calculations and image matrix manipulations were performed using SPM8 running on MATLAB R2007a software (MathWorks, Natick, MA). MR imaging data were analyzed using DARTEL as a toolbox for SPM8 to create a set of group-specific templates. The brain images were segmented, normalized, and modulated by using these templates. The output images were still in the average brain space. Additional warping from the Montreal Neurologic Institute space was given to the brain images. Then, gray matter probability values were smoothed by using an 8-mm full-width at half-maximum Gaussian kernel.

4.3.3. DTI procedure

The DTI data sets were analyzed using DtiStudio (Jiang et al., 2006). The diffusion tensor parameters were calculated on a pixel-by-pixel basis, and FA and MD map and $b=0$ image were calculated according to Wakana et al. (2004).

4.3.4. SPM analysis

To estimate the relationships between brain morphology and % PPI, FA and MD images were analyzed using an optimized VBM technique. The data were analyzed using SPM5 software running on MATLAB 7.0. The images were processed using an optimized VBM script. The details of this process are described elsewhere (Good et al., 2001). First, each individual 3D-T1 image was coregistered and resliced to its own $b=0$ image. Next, the coregistered 3D-T1 image was normalized to the "avg152T1" image regarded as the anatomically standard image in SPM5. Finally, the transformation matrix was applied to FA and MD maps. Further, to avoid the effect of diffusivity of cerebrospinal fluid (CSF), MD images were masked with the CSF image derived from the segmented individual 3D-T1 image. Each map was then spatially smoothed with a 6-mm full-width at half-maximum Gaussian kernel in order to decrease spatial noise and compensate for the inexactitude of normalization following the "rule of thumb" developed for fMRI and PET studies (Snook et al., 2007).

4.3.5. Tract-based spatial statistics (TBSS) analysis

The processing technique known as "tract-based spatial statistics (TBSS) analysis" projects DTI data onto a common pseudo-anatomical skeleton instead of trying to match each and every voxel in different subjects, and therefore does not need smoothing (Smith et al., 2006). TBSS is available as part of the FSL 4.1 software package (Smith et al., 2004). The TBSS script runs a nonlinear registration, aligning all FA images to the FMRIB58_FA template, which is supplied with FSL. The script then takes the target and affine-aligns it into a 1 × 1 × 1 mm MNI152 space. Once this is done, each subject's FA image has the nonlinear transform to the target and then the affine transform to MNI152 space is applied, resulting in a transformation of the original FA image into MNI152 space. Next, TBSS creates the mean of all aligned FA images and applies thinning of the local tract structure to create a skeletonized mean FA image. In order to exclude areas of low FA and/or high intersubject variability from a statistical analysis, TBSS thresholds a mean FA skeleton with a certain FA value, typically 0.2. The resulting binary skeleton mask is a pseudo-anatomical representation of the main fiber tracks, and defines the set of voxels used in all subsequent processing. Finally, TBSS projects each subject's aligned FA image onto the skeleton. This results in skeletonized FA data. It is this file that is used for the voxelwise statistics.

4.3.6. Statistical analysis

Statistical analyses were performed using SPM5 software (Welcome Department of Imaging Neuroscience, London, UK). Correlations between regional gray matter volume and % PPI with 86 and 90 dB of prepulse were assessed using the subjects' age, length of education, and whole brain volume as nuisance variables, and FA and MD value maps and % PPI

were assessed using age and education year as nuisance variables. Only correlations that met these criteria were deemed significant. In this case, a seed level of $p<0.001$ (uncorrected) and a cluster level of $p<0.05$ (uncorrected) were selected.

Skeletonized FA data were analyzed for revealing correlations with % PPI, controlling for age, using the FSL "Threshold-Free Cluster Enhancement (TFCE)" option in "randomise" with 5000 permutations, the script of which uses a permutation-based statistical inference that does not rely on a Gaussian distribution of voxels, and is run without having to define an initial cluster-forming threshold or carry out a large amount of data smoothing (Nichols and Holmes, 2002; Smith and Nichols, 2009). The significance level was set at the p-value of less than 0.05 with FWE rate correction for multiple comparisons.

Acknowledgments

This study was supported by Health and Labor Sciences Research Grants (Comprehensive Research on Disability, Health, and Welfare), Intramural Research Grant (24-11) for Neurological and Psychiatric Disorders of NCNP (M.O. and H.K.), "Understanding of molecular and environmental bases for brain health" carried out under the Strategic Research Program for Brain Sciences by the Ministry of Education, Culture, Sports, Science and Technology of Japan, and a grant from Core Research of Evolutional Science & Technology (CREST), Japan Science and Technology Agency (JST) (H.K.)

REFERENCES

Ashburner, J., 2007. A fast diffeomorphic image registration algorithm. NeuroImage 38, 95–113.

Braff, D.L., Geyer, M.A., Swerdlow, N.R., 2001. Human studies of prepulse inhibition of startle: normal subjects, patient groups, and pharmacological studies. Psychopharmacology (Berl) 156, 234–258.

Cadenhead, K.S., Braff, D.L., 1999. Schizophrenia spectrum disorders. In: Dawson, M.E., Schell, A.M., Bohmelt, A.H. (Eds.), Startle Modification: Implications for Neuroscience. Cognitive Science, and Clinical Science. Cambridge University Press, Cambridge, pp. 231–244.

Fendt, M., Liang, L., Yeomans, J.S., 2001. Brain stem circuits mediating prepulse inhibition of the startle reflex. Psychopharmacology 156, 216–224.

Good, C.D., Johnsrude, I., Ashburner, J., Henson, R.N.A., Friston, K.J., Frackowiak, R.S.J., 2001. Cerebral asymmetry and the effect of sex and handedness on brain structure: a voxel-based morphometric analysis of 465 normal adult human brains. NeuroImage 14, 685–700.

Hazlett, E.A., Buchsbaum, M.S., Haznedar, M.M., Singer, M.B., Germans, M.K., Schnur, D.B., Jimenez, E.A., Buchsbaum, B.R., Troyer, B.T., 1998. Prefrontal cortex glucose metabolism and startle eyeblink modification abnormalities in unmedicated schizophrenia patients. Psychophysiology 35, 186–198.

Hazlett, E.A., Buchsbaum, M.S., Tang, C.Y., Fleischman, M.B., Wei, T.C., Byne, W., Haznedar, M.M., 2001. Thalamic activation during an attention-to-prepulse startle modification paradigm: a functional MRI study. Biol. Psychiatry 50, 281–291.

Hazlett, E.A., Buchsbaum, M.S., Zhang, J., Newmark, R.E., Glanton, C.F., Zelmanova, Y., Haznedar, M.M., Chu, K.W., Nenadic, I., Kemether, L.J., Tang, C.Y., New, A.S., Siever, L.J., 2008. Frontal–striatal–thalamic mediodorsal nucleus dysfunction in schizophrenia-spectrum patients during sensorimotor gating. NeuroImage 42, 1164–1177.

Jiang, H., van Zijil, P.C., Kim, J., Pearlson, G.D., Mori, S., 2006. DtiStudio: resource program for diffusion tensor computation and fiber bundle tracking. Comput. Methods Programs Biomed. 81, 106–116.

Koch, M, Schnitzler, H, 1997. The acoustic startle response in rats: circuits mediating evocation, inhibition and potentiation. Behav. Brain Res. 89, 35–49.

Kumari, V., Aasen, I., Sharma, T., 2004. Sex differences in prepulse inhibition deficits in chronic schizophrenia. Schizophr. Res. 69, 219–235.

Kumari, V., Antonova, E., Geyer, M.A., 2008a. Prepulse inhibition and "psychosis-proneness" in healthy individuals: an fMRI study. Eur. Psychiatry 23, 274–280.

Kumari, V., Antonova, E., Geyer, M.A., Ffytche, D., Williams, S.C., Sharma, T., 2007. A fMRI investigation of startle gating deficits in schizophrenia patients treated with typical or atypical antipsychotics. Int. J. Neuropsychopharmacol. 10, 463–477.

Kumari, V., Antonova, E., Zachariah, E., Galea, A., Aasen, I., Ettinger, U., Mitterschiffthaler, M.T., Sharma, T., 2005. Structural brain correlates of prepulse inhibition of the acoustic startle response in healthy humans. NeuroImage 26, 1052–1058.

Kumari, V., Fannon, D., Geyer, M.A., Premkumar, P., Antonova, E., Simmons, A., Kuipers, E., 2008b. Cortical grey matter volume and sensorimotor gating in schizophrenia. Cortex 44, 1206–1214.

Kumari, V., Gray, J.A., Geyer, M.A., Ffytche, D., Mitterschiffthaler, M.T., Vythelingum, G.N., Williams, S.C.R., Simmons, A., Sharma, T., 2003. Neural correlates of prepulse inhibition in normal and schizophrenic subjects: a functional MRI Study. Psychiatry Res.: NeuroImage 122, 99–113.

Kunugi, H., Tanaka, M., Hori, H., Hashimoto, R., Saitoh, O., Hironaka, N., 2007. Prepulse inhibition of acoustic startle in Japanese patients with chronic schizophrenia. Neurosci. Res. 59, 23–28.

McGhie, A, Chapman, J., 1961. Disorders of attention and perception in early schizophrenia. Br. J. Med. Psychol. 34, 103–116.

Moriwaki, M., Kishi, T., Takahashi, H., Hashimoto, R., Kawashima, K., Okochi, T., Kitajima, T., Furukawa, O., Fujita, K., Takeda, M., Iwata, N., 2009. Prepulse inhibition of the startle response with chronic schizophrenia: a replication study. Neurosci. Res. 65, 259–262.

Nichols, T.E., Holmes, A.P., 2002. Nonparametric permutation tests for functional neuroimaging: a primer with examples. Hum. Brain. Mapp. 15, 1–25.

Otsubo, T., Tanaka, K., Koda, R., Shinoda, J., Sano, N., Tanaka, S., Aoyama, H., Mimura, M., Kamijima, K., 2005. Reliability and validity of Japanese version of the Mini-International Neuropsychiatric Interview. Psychiatry Clin. Neurosci. 59, 517–526.

Perry, W., Minassian, A., Feifel, D., 2004. Prepulse inhibition in patients with non-psychotic major depressive disorder. J. Affect. Disord. 81, 179–184.

Sheehan, D.V., Lecrubier, Y., Sheehan, K.H., Amorim, P., Janavs, J., Weiller, E., Hergueta, T., Baker, R., Dunbar, G.C., 1998. The Mini-International Neuropsychiatric Interview (M.I.N.I.): the development and validation of a structured diagnostic psychiatric interview for DSM-IV and ICD-10. J. Clin. Psychiatry 59, 22–57.

Smith, S.M., Jenkinson, M., Johansen-Berg, H., Rueckert, D., Nichols, T.E., Mackay, C.E., Watkins, K.E., Ciccarelli, O., Cader, M.Z., Matthews, P.M., Behrens, T.E., 2006. Tract-based

spatial statistics: voxelwise analysis of multi-subject diffusion data. NeuroImage 31, 1487–1505.

Smith, S.M., Jenkinson, M., Woolrich, M.W., Beckmann, C.F., Behrens, T.E., Johansen-Berg, H., Bannister, P.R., De Luca, M., Drobnjak, I., Flitney, D.E., Niazy, R.K., Saunders, J., Vickers, J., Zhang, Y., De Stefano, N., Brady, J.M., Matthews, P.M., 2004. Advances in functional and structural MR image analysis and implementation as FSL. NeuroImage 23 (1), S208–219.

Smith, S.M., Nichols, T.E., 2009. Threshold-free cluster enhancement: addressing problems of smoothing, threshold dependence and localisation in cluster inference. NeuroImage 44, 83–98.

Snook, L., Plewes, C., Beaulieu, C., 2007. Voxel based versus region of interest analysis in diffusion tensor imaging of neurodevelopment. NeuroImage 34, 243–252.

Swerdlow, N.R., Geyer, M.A., 1998. Using an animal model of deficient sensorimotor gating to study the pathophysiology and new treatments of schizophrenia. Schizophrenia Bull. 24, 285–301.

Swerdlow, N.R., Geyer, M.A., Braff, D.L., 2001. Neural circuit regulation of prepulse inhibition of startle in the rat: current knowledge and future challenges. Psychopharmacology 156, 194–215.

Swerdlow, N.R., Hartman, P.L., Auerbach, P.P., 1997. Changes in sensorimotor inhibition across the menstrual cycle: implications for neuropsychiatric disorders. Biol. Psychiatry 41, 452–460.

Swerdlow, N.R., Weber, M., Qu, Y., Light, G.A., Braff, D.L., 2008. Realistic expectations of prepulse inhibition in translational models for schizophrenia research. Psychopharmacology (Berl) 199, 331–388.

Takahashi, H., Iwase, M., Ishii, R., Ohi, K., Fukumoto, M., Azechi, M., Ikezawa, K., Kurimoto, R., Canuet, L., Nakahachi, T., Iike, N., Tagami, S., Morihara, T., Okochi, M., Tanaka, T., Kazui, H, Yoshida, T, Tanimukai, H, Yasuda, Y, Kudo, T, Hashimoto, R, Takeda, M., 2008. Impaired prepulse inhibition and habituation of acoustic startle response in Japanese patients with schizophrenia. Neurosci. Res. 62, 187–194.

Wakana, S., Jiang, H., Nagae-Poetscher, L.M., van Zijl, P.C., Mori, S., 2004. Fiber tract-based atlas of human white matter anatomy. Radiology 230, 77–87.

Yassa, M.A., Stark, C.E., 2009. A quantitative evaluation of cross-participant registration techniques for MRI studies of the medial temporal lobe. NeuroImage 44, 319–327.

Magnetic Resonance Imaging xxx (2013) xxx–xxx

Contents lists available at SciVerse ScienceDirect

Magnetic Resonance Imaging

journal homepage: www.mrijournal.com

Abnormalities of cerebral blood flow in multiple sclerosis: A pseudocontinuous arterial spin labeling MRI study☆

Miho Ota [a,*], Noriko Sato [b], Yasuhiro Nakata [b], Kimiteru Ito [b], Kouhei Kamiya [b], Norihide Maikusa [c], Masafumi Ogawa [d], Tomoko Okamoto [d], Satoko Obu [a], Takamasa Noda [e], Manabu Araki [d], Takashi Yamamura [f], Hiroshi Kunugi [a]

[a] Department of Mental Disorder Research, National Institute of Neuroscience, National Center of Neurology and Psychiatry, 4-1-1, Ogawa-Higashi, Kodaira, Tokyo 187-8502, Japan
[b] Department of Radiology, National Center of Neurology and Psychiatry, 4-1-1, Ogawa-Higashi, Kodaira, Tokyo 187-8551, Japan
[c] Department of Imaging Neuroinformatics, Integrative Brain Imaging Center, National Center Hospital of Neurology and Psychiatry, 4-1-1 Ogawa-Higashi, Kodaira, Tokyo 187-8502, Japan
[d] Department of Neurology, National Center of Neurology and Psychiatry, 4-1-1, Ogawa-Higashi, Kodaira, Tokyo 187-8551, Japan
[e] Department of Psychiatry, National Center of Neurology and Psychiatry, 4-1-1, Ogawa-Higashi, Kodaira, Tokyo 187-8551, Japan
[f] Department of Immunology, National Institute of Neuroscience, National Center of Neurology and Psychiatry, 4-1-1, Ogawa-Higashi, Kodaira, Tokyo 187-8502, Japan

ARTICLE INFO

Article history:
Received 20 September 2012
Revised 30 January 2013
Accepted 9 March 2013
Available online xxxx

Keywords:
Cerebral blood flow
Multiple sclerosis
Pseudocontinuous arterial spin labeling
T2-hyperintense lesion

ABSTRACT

Arterial spin labeling (ASL) is a noninvasive technique that can measure cerebral blood flow (CBF). To our knowledge, there is no study that examined regional CBF of multiple sclerosis (MS) patients by using this technique. The present study assessed the relationship between clinical presentations and functional imaging data in MS using pseudocontinuous arterial spin labeling (pCASL). Twenty-seven patients with MS and 24 healthy volunteers underwent magnetic resonance imaging and pCASL to assess CBF. Differences in CBF between the two groups and the relationships of CBF values with the T2-hyperintense volume were evaluated. Compared to the healthy volunteers, reduced CBF was found in the bilateral thalami and right frontal region of the MS patients. The volume of the T2-hyperintense lesion was negatively correlated with regional CBF in some areas, such as both thalami. Our results suggest that demyelinated lesions in MS mainly have a remote effect on the thalamus and that the measurement of CBF using ASL could be an objective marker for monitoring disease activity in MS.

1. Introduction

Multiple sclerosis (MS) is a common autoimmune disorder of the central nervous system (CNS) characterized by inflammatory demyelination and secondary axonal degeneration. Although MS has classically been thought of as a typical white matter disorder, the involvement of gray matter regions in the demyelinating process was acknowledged in early pathology studies [1–5], and some hypotheses have been put forward that have explored possible pathogenic processes leading to gray matter damage. These processes could be either primary (arising within gray matter regions) or secondary (pathological changes in gray matter regions that result from continuing damage in the cerebral white matter) and might be intricately connected with each other [6].

Positron emission tomography (PET), single photon emission computed tomography (SPECT) and dynamic susceptibility contrast (DSC)-enhanced magnetic resonance imaging (MRI) have been used to investigate cerebral metabolic rate, cerebral blood flow (CBF) and cerebral perfusion in MS, respectively. Such imaging techniques have shown significant decreases in areas of white matter, cortical gray matter, subcortical gray matter and normal-appearing white matter [7–16]. However, due to the dissemination of MS lesions in space and time, potential markers for determining their outcomes are poorly understood.

Arterial spin labeling (ASL) MRI is a noninvasive technique that can measure CBF. ASL MRI has two major categories: continuous ASL (CASL) and pulsed ASL (PASL) [17]. The CASL technique uses continuous adiabatic inversion, whereas PASL uses a single inversion pulse. Due to the long steady-state tagging, this technique often has high power disposition and sometimes requires a second radio-frequency (RF) coil for spin labeling [18,19]. Therefore, it has not been widely used compared with PASL, which is simpler in implementation. The recently developed pseudocontinuous ASL (pCASL) MRI is an intermediate technique between CASL and PASL [20–22]. This technique uses a series of discrete RF pulses to mimic the CASL method for spin labeling and brings the potential of combining the merits of PASL, including less hardware demand and higher tagging efficiency, and CASL, which include a longer tagging bolus and thus a higher signal-to-noise ratio.

☆ Conflict of interest: None.

* Corresponding author. Tel.: +81 42 341 2712; fax: +81 42 346 2094.
E-mail address: ota@ncnp.go.jp (M. Ota).

0730-725X/$ – see front matter © 2013 Elsevier Inc. All rights reserved.
http://dx.doi.org/10.1016/j.mri.2013.03.016

ASL measures CBF by taking advantage of arterial water as a freely diffusible tracer, avoiding the need for gadolinium or radioactive ligands; thus, ASL would be a noninvasive and repeatable method of measuring CBF. The ASL technique could be used in place of DSC, PET and SPECT for the examination of neurologic disorders.

We hypothesized that decreased CBF measured by pCASL would, in reflecting neuronal and axonal loss, be associated with the clinical course and disabling forms of MS. In the present study, we assessed the relationship between clinical presentations and functional imaging data in MS using pCASL.

2. Material and methods

2.1. Participant selection

The subjects were 27 patients with MS and 24 healthy controls matched for age, gender and whole brain volume. MS was diagnosed by using previously defined criteria [23]. One female patient out of 27 was the primary progressive MS, and 8 out of 27 (all of them were female, mean age = 47.3 ± 12.9 years) were the secondary progressive MS. No subject had a previous history of any other significant central nervous or systemic autoimmune conditions. The healthy controls were all volunteers without any confirmed neuropsychiatric or major medical illness. All MS subjects underwent a neurological examination to evaluate their Expanded Disability Status Scale (EDSS) scores [24]. The demographic and clinical data of the subjects are shown in Table 1. The study protocol was approved by the Ethics Committee of the National Center of Neurology and Psychiatry, Japan. Informed consent for participation in the study was obtained from all subjects.

2.2. MRI data acquisition and processing

Experiments were performed on a 3-T MR system (Philips Medical Systems, Best, the Netherlands). High spatial resolution, 3-dimensional (3D) T1-weighted images were used for morphometric study. 3D T1-weighted images were acquired in the sagittal plane [repetition time (TR)/echo time (TE), 7.18/3.46; flip angle, 10°; effective section thickness, 0.6 mm; slab thickness, 180 mm; matrix, 384 × 384; field of view (FOV), 261 × 261 mm; number of signals acquired, 1], yielding 300 contiguous slices through the brain. In addition to 3D T1-weighted images, we acquired axial T2-weighted turbo spin echo images (TR/TE, 4507/80; slice thickness, 3 mm; intersection gap, 1.5 mm; matrix, 640 × 640; FOV, 230 × 230 mm; number of signals acquired, 1) and axial fluid-attenuated inversion recovery (FLAIR) images (TR/TE/inversion time, 10,000/120/2650 ms; slice thickness, 3 mm; intersection gap, 1.5 mm; matrix, 512 × 512; FOV, 230 × 230 mm; number of signals acquired, 1). The imaging parameters for all of the pCASL experiments were identical: single-shot gradient-echo echo planar imaging (EPI) in combination with parallel imaging (SENSE factor 2.0), FOV = 240 × 240, matrix = 64 × 64, voxel size = 3.75 × 3.75 mm, 20 slices acquired in ascending order, slice thickness = 7 mm, 1-mm gap between slices, labeling duration = 1650 ms, post spin labeling delay = 1520 ms, TR = 4000 ms, TE = 12 ms, time interval between consecutive slice acquisitions = 32.0 ms, RF duration = 0.5 ms, pause between RF pulses = 0.5 ms, labeling pulse flip angle = 18°, bandwidth = 3.3 kHz/pixel, echo train length = 35. Thirty-two pairs of control/label images were acquired and averaged. The scan duration was 4:24. For measurement of the magnetization of arterial blood and also for segmentation purposes, an EPI M0 image was acquired separately with the same geometry and the same imaging parameters as the pCASL without labeling.

Table 1
Characteristics of the study sample.

	Healthy volunteers	Multiple sclerosis patients
Male/female	7/17	7/20
Age	38.3 ± 13.2	42.7 ± 13.6
Whole brain volume (L)	1.1 ± 0.1	1.1 ± 0.1
Duration of illness		10.6 ± 9.2
EDSS		4.4 ± 2.5
T2-hyperintense lesion volume (cm^3)		3.4 ± 4.0

2.3. Postprocessing of the ASL data

Because pCASL and M0 images were acquired separately, both image signal intensities were corrected for data scaling. Corrected data were transferred to a workstation and analyzed using ASLtbx software working on Matlab (Math Works, Natick, MA, USA) [25]. For the CBF calculations, we added the attenuation correction for the transversal relaxation rate of gray matter to the original equation as shown:

$$\begin{aligned}\text{CBF (ml/100 g/min)} &= (6000 * \text{delM} * \text{lamb}) \\ &* \exp(\text{TE}/T^{*}_{2.\text{gm}}/[2 * \text{alp} * T_{1,\text{blood}} * \text{M0WM}\{\exp(-w/T_{1,\text{blood}}) \\ &-\exp(-(\text{tau}+w)/T_{1,\text{blood}})\}],\end{aligned}$$

Where delM is the difference signal between the control and label acquisitions, lamb is the blood/tissue water partition coefficient, $T_{1,blood}$ is the longitudinal relaxation time of blood, tau is the labeling time, w is the post labeling delay time, TE is the echo time and $T^{*}_{2.gm}$ is the transversal relaxation time of gray matter (assumed to be 44.2 ms) [26]. Alp is the labeling efficiency, and M0WM is the average intensity in the control image within the white matter that was derived from the segmented M0 white matter image calculated using Statistical Parametric Mapping 5 software (SPM5; Wellcome Department of Imaging Neuroscience, London, UK) running on Matlab 7.0. The parameters used in this study were alp = 0.85 (assumed) [17], $T_{1,blood}$ = 1664 ms (assumed) [27], λ = 0.9 g/ml (assumed) [28], tau = 1.65 s (calculated) and w = 1525 (calculated) ms.

The mean CBF image derived using the ASLtbx software contained some spike noise, and thus, a median filter (a nonlinear digital filtering technique) was used in this study. In median filtering, the neighboring pixels are ranked according to the intensity, and the median value becomes the new value for the central pixel. Since the slice gap that we used was somewhat large, simple 2D median filtering was used. Fig. 1 illustrated the image from the ASL sequence in a single subject. To evaluate CBF voxel-basically, mean CBF images were normalized to the standard space. On the occasion of normalization, each individual 3D-T1 image was first coregistered and resliced to its own M0 image. Next, the coregistered 3D-T1 image was normalized to the "avg152T1" image regarded as the anatomically standard image in SPM5, and then the transformation matrix was applied to the FA maps to normalize them to the standard space. The spatially normalized images were resliced with a final voxel size of approximately 4 × 4 × 8 mm^3. Each map was then spatially smoothed with a 4-mm full-width at half-maximum Gaussian kernel in order to decrease spatial noise and compensate for the inexactitude of normalization.

2.4. Measure of volume of T2-hyperintense lesion

The T2-weighted data and FLAIR images for each subject were transferred to the workstation. To measure the accurate volume of the T2-hyperintense lesion, individual T2-weighted data and FLAIR data sets were analyzed using QBrain@1.1 [22]. The volume

Please cite this article as: Ota M, et al, Abnormalities of cerebral blood flow in multiple sclerosis: A pseudocontinuous arterial spin labeling MRI study, Magn Reson Imaging (2013), http://dx.doi.org/10.1016/j.mri.2013.03.016

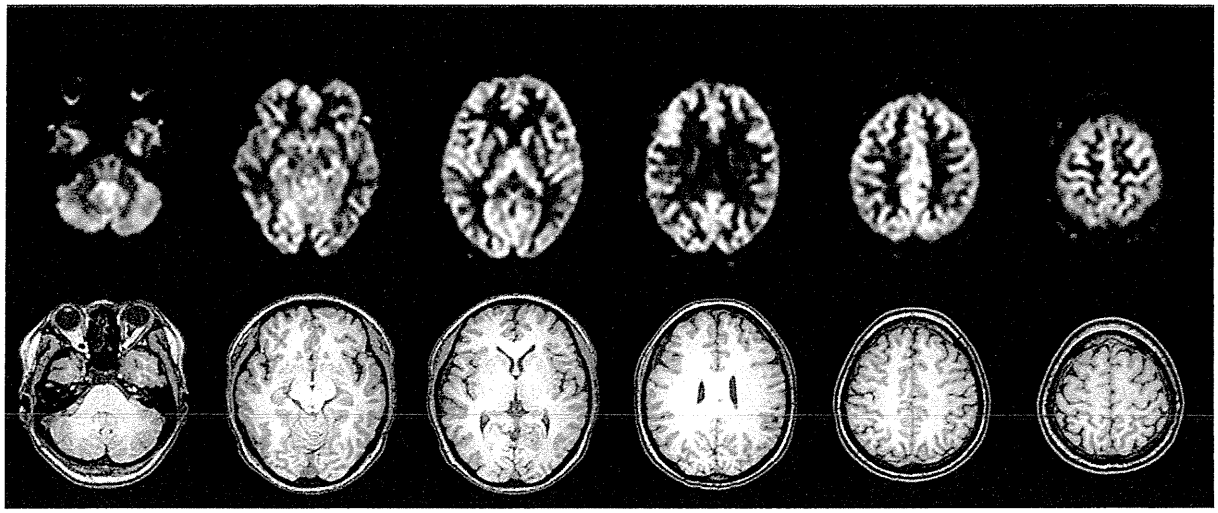

Fig. 1. The upper row showed the typical example of ASL CBF maps acquired in a single healthy volunteer, and lower row showed corresponding slices of T1-weighted image.

quantifications were first performed with manual segmentation and second with the fully automatic segmentation algorithms. Using the software, the T2-hyperintense lesions can be reliably quantified in the milliliter range.

2.5. Measure of whole brain volume

We regarded the gray matter volume plus white matter volume as the whole brain volume. The values of gray and white matter volumes of individual subjects were extracted with the Easy Volume toolbox [29] running on Matlab 7.0. The gray matter and white matter volume images were derived from the segmented 3D-T1 image calculated using SPM5.

2.6. Statistical analysis

We first evaluated the correlations among the EDSS score, age, duration of illness and the ratio of T2-hyperintense lesion volume/whole brain volume in the MS patients by using Pearson's correlation analysis. Statistical analyses were performed using SPSS Statistics for Windows 17.0 software (SPSS, Tokyo, Japan).

Next, statistical analyses for the CBF were performed using SPM5 software. We evaluated the difference in regional CBF (rCBF) between the MS patients and healthy subjects using age and gender as nuisance variables. Only correlations that met the following criteria were deemed statistically significant: seed levels of $P < .05$ [false discovery rate (FDR) corrected] and a cluster level of $P < .05$ (uncorrected).

Next, correlations between rCBF values and the ratio of T2-hyperintense lesion volume/whole brain volume and between rCBF values and EDSS scores were assessed using age, gender and duration of illness as nuisance variables. Only correlations that met the following criteria were deemed significant: a seed level of $P < .001$ (uncorrected) and a cluster level of $P < .05$ (uncorrected).

Finally, we highlighted the influence of the T2-hyperintense lesion on the CBF. We masked the latter results with the regions for which the results of the former analysis were regarded as significant. This mask was based on partially the same data of the latter analysis; there

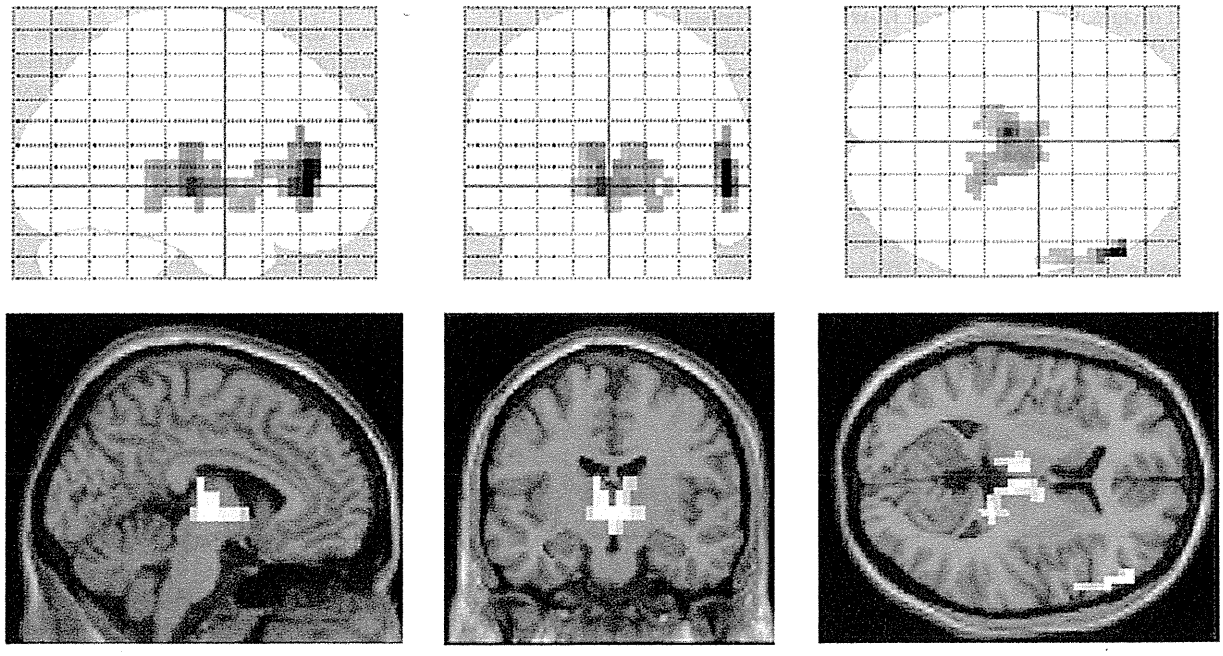

Fig. 2. There were significant reductions of CBF in the right prefrontal cortex and bilateral thalami in the MS patients compared to the healthy controls [$P < .05$ (FDR corrected)].

Please cite this article as: Ota M, et al, Abnormalities of cerebral blood flow in multiple sclerosis: A pseudocontinuous arterial spin labeling MRI study, Magn Reson Imaging (2013), http://dx.doi.org/10.1016/j.mri.2013.03.016

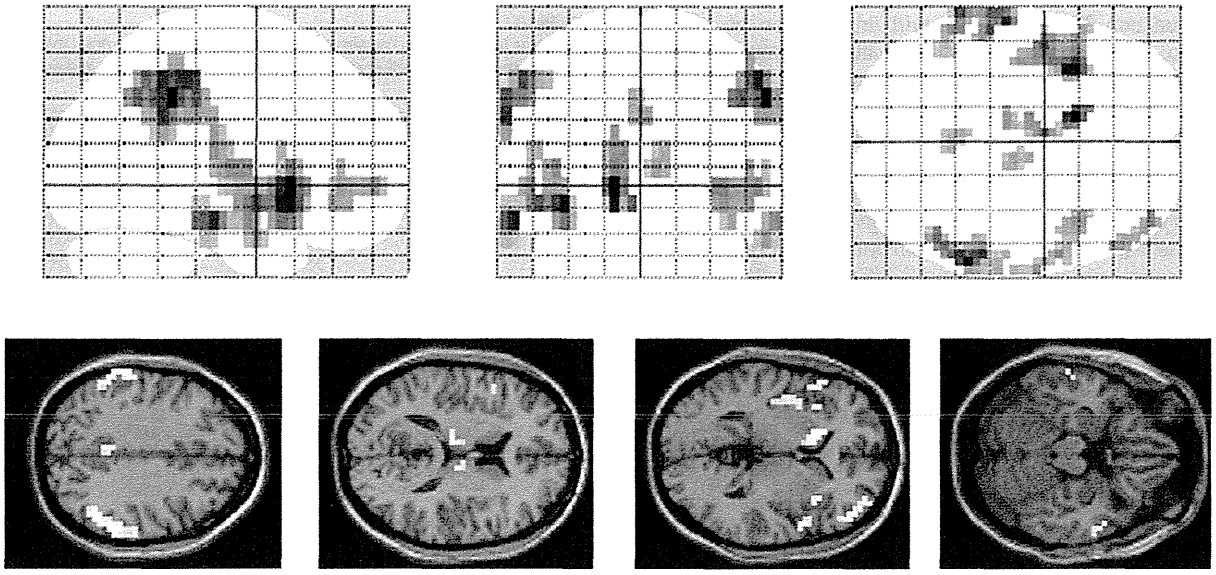

Fig. 3. There were negative correlations between the T2-hyperintense lesion volume/whole brain volume ratio and the regional CBF values in several areas throughout the brain in the MS patients ($P < .001$, uncorrected).

existed a multiple testing problem. So, we use the formal thresholding (e.g., FDR) that accounts for this multiplicity [30]. The mask applied the seed levels of $P < .05$ (FDR corrected) as statistically significant.

3. Results

There were no significant correlations between any combinations of two factors of EDSS score, age, duration of illness and the ratio of T2-hyperintense lesion volume/whole brain volume in the MS patients (data not shown). There were significant reductions of CBF in the bilateral thalami and right frontal region of the MS patients compared to the healthy controls (Fig. 2 and Table 2).

There was no increase of CBF in MS patients (data not shown). In the MS patient group, the T2-hyperintense lesion volume/whole brain volume ratio was negatively correlated with rCBF values in the right frontal region, both parietal and temporal regions, both insulae, the left caudate, both thalami and both posterior cinguli (Fig. 3 and Table 3). There were no differences of regional CBF between relapsing–remitting MS patients and secondary progressive MS patients (data not shown).

In contrast, there was no correlation between the EDSS scores and rCBF values (data not shown). There were significant negative correlations between the ratio of the T2-hyperintense lesion volume to whole brain volume and CBF in both thalami when we masked the second results with the regions in which the results of the first analysis were regarded as significant (Fig. 4).

4. Discussion

To our knowledge, this is the first evaluation of the possible relationships between clinical presentations of MS and CBF using pCASL. By using the pCASL technique, we found significant correlations between the volume of T2-hyperintense lesions and the rCBF values. In particular, CBF in the thalamus was significantly decreased in the patients with MS compared to that of the healthy subjects, and thalamic CBF was correlated with the volume of T2-hyperintense lesion.

There were a few studies of MS using CASL and PASL [14,31]. One study using the CASL showed the reduction of thalamic CBF in MS; however, they did not evaluate the correlation between the volume of T2-hyperintense lesions and the rCBF values [14]. On the other hand, the study using PASL showed not the correlation between them but the correlation between the volume of lesions and mean cortical CBF [31]. These facts may indicate that the CBF study using pCASL calculates the rigorous CBF value. In addition, these studies, including our study, did not show the correlation between the EDSS and rCBF. This may result from the fact that the EDSS mainly focused on the ambulatory ability, not on the higher brain function, so the change of cortical CBF in MS did not reflect the EDSS score. In recent years, the MS Functional Composite (MSFC) was proposed for a new multidimensional clinical outcome measure of MS [32]. The MSFC comprises quantitative functional measures of three key clinical dimensions of MS: leg function ambulation, arm/hand function and

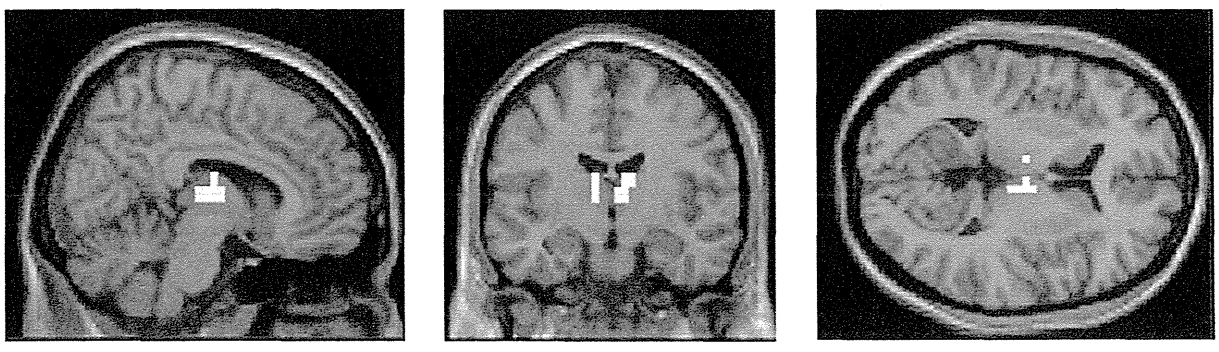

Fig. 4. When the correlation analysis was restricted in both thalami where the CBF reduction was detected in the MS patients, there were significant negative correlations between the T2-hyperintense lesion volume/whole brain volume ratio and the CBF values.

Please cite this article as: Ota M, et al, Abnormalities of cerebral blood flow in multiple sclerosis: A pseudocontinuous arterial spin labeling MRI study, Magn Reson Imaging (2013), http://dx.doi.org/10.1016/j.mri.2013.03.016

cognitive function. Further studies with information on MSFC are necessary to address this issue. Additionally, we showed the CBF reduction of the patients with MS in the inferior prefrontal cortex. Previous study showed that MS patients with long duration of disease showed atrophy of the thalami and inferior frontal gyrus [33]. The participants in this study showed relatively long disease duration (Table 1); then the CBF of the patients would show the reduction.

We also found negative correlations between the ratio of the T2-hyperintense lesion volume/whole brain volume and regional CBF in several areas throughout the brain in the MS patients. We focused on volume and not on distribution of the T2-hyperintense lesion in the whole brain, and therefore, the relationship between the volume of lesion and the regional CBF was not examined. However, some previous studies showed reduced metabolism in the prefrontal, parietal and occipital cortex and hippocampus, thalamus, putamen and caudate in MS [7,8,13,14], and those findings are compatible with our results.

Regarding the thalamus, an MRI study of MS patients reported a decrease in thalamic volume and *N*-acetyl aspartate [34]. Those authors also identified the thalamic neuronal loss in MS patients by postmortem examination. Evaluations of the metabolism and perfusion in the brains of patients with MS have also revealed hypometabolism and hypoperfusion in the thalamus [9,12,14] Furthermore, PET metabolic studies suggest a possible correlation between thalamic hypometabolism and cognitive impairment [7], memory disturbance [13] and the volume of deep white matter lesions [8]. The decreased thalamic CBF observed in our study is consistent with the findings of these previous studies. Another study using diffusion tensor imaging revealed the fine neural networks in the CNS [35]. The thalamus is regarded as the central relay station of the brain, and the reciprocal influence between the thalamus and its associated areas has been well described [36]. The decreased CBF that we observed in the thalamus of the MS patients may be an indication of a disconnection between cortical regions and subcortical relay systems due to the lesion process in MS.

There were some limitations of this study. First, we dealt with the whole brain CBF images, including the gray matter and white matter, voxel-basically. However, we could not detect the white matter CBF change. Previous study showed that the female patients with MS showed the change of white matter compared with men, while gender did not impact gray matter atrophy [33]. Along with the dissemination of MS lesions in space and time, co-gender participants may influence on our results. Further work with single-gender MS patients will be necessary to confirm our results. Second, we did not classify the participants into the three subgroups of MS. The subgroups of MS were defined by the clinical course of illness, and this is not for a cross-sectional study containing the first episode of illness. Not only our study but also two previous cross-sectional studies using ASL also did not show the differences among the subgroups of MS [14,31]. Further longitudinal work would show the difference among the subgroups. A third limitation of the present study is that we did not eliminate the effect of immunomodulating treatment on CBF. Further work with drug-free MS patients will be necessary to confirm our results.

In conclusion, our findings indicate that the noninvasive pCASL is a useful technique which demonstrated that regional CBF values are closely related to the brain lesions in MS. In addition, our results suggest that the demyelinating lesions in MS mainly have a remote effect on the function of the thalamus. Measurement of CBF by pCASL MRI has the potential to be an objective marker for monitoring disease activity in MS (Tables 2 and 3).

Table 2
Regions that showed significant differences in cerebral blood flow between the patients with multiple sclerosis ($n = 27$) and healthy controls ($n = 24$) using age and gender as nuisance variables.

Cluster size	*Z* score	*x*	*y*	*z*	Brain region
35	5.17	56	40	8	Right frontal lobe
114	4.61	−4	−16	0	Left thalamus
	4	8	−16	0	Right thalamus

Table 3
Regions of significant negative correlations between cerebral blood flow and T2-hyperintense lesion volume in MS patients using age, gender and duration of illness as nuisance variables.

Cluster size	*Z* score	*x*	*y*	*z*	Brain region
16	3.62	40	56	0	Right frontal lobe
35	3.98	−64	−44	32	Left parietal lobe
49	4.33	60	−40	40	Right parietal lobe
11	4.17	−60	−20	−16	Left temporal lobe
9	3.61	64	−4	−16	Right temporal lobe
68	4.29	−36	16	−8	Left insula
24	3.59	56	8	0	Right insula
23	4.59	−12	16	0	Left caudate
11	3.55	−12	−8	8	Left thalamus
9	3.42	8	−16	8	Right thalamus
12	3.37	4	−48	32	Right posterior cingulate
	3.33	−4	−44	40	Left posterior cingulate

Acknowledgments

We are grateful to Ms. Yuriko Suzuki at Philips for helpful discussions. This study was supported by Health and Labour Sciences Research Grants (Comprehensive Research on Disability, Health, and Welfare, #H23-seisin-young scientist 013; #H21-kokoro-002), an Intramural Research Grant for Neurological and Psychiatric Disorders of NCNP and "Understanding of molecular and environmental bases for brain health" carried out under the Strategic Research Program for Brain Sciences of the Ministry of Education, Culture, Sports, Science and Technology of Japan.

References

[1] Brownell B, Hughes JT. The distribution of plaques in the cerebrum in multiple sclerosis. J Neurol Neurosurg Psychiatry 1962;25:315–20.
[2] Dawson JW. The histology of multiple sclerosis. Trans R Soc (Edinb) 1916;50:517–740.
[3] Dinkler M. Zur Kasuistik der multiplen Herdsklerose des Gehirns und Ruckenmarks. Deuts Zeits f Nervenheilk 1904;26:233–47.
[4] Sander M. Hirnrindenbefunde bei multipler Sklerose. Monatschrift Psychiatrie Neurol 1898;IV:427–36.
[5] Schob F. Ein Beitrag zur pathologischen Anatomie der multiplen Sklerose. Monatschrift Psychiatrie Neurol 1907;22:62–87.
[6] Geurts JJ, Barkhof F. Grey matter pathology in multiple sclerosis. Lancet Neurol 2008;7:841–51.
[7] Blinkenberg M, Rune K, Jensen CV, Ravnborg M, Kyllingsbaek S, Holm S, et al. Cortical cerebral metabolism correlates with MRI lesion load and cognitive dysfunction in MS. Neurology 2000;54:558–64.
[8] Derache N, Marié RM, Constans JM, Defer GL. Reduced thalamic and cerebellar rest metabolism in relapsing-remitting multiple sclerosis, a positron emission tomography study: correlations to lesion load. J Neurol Sci 2006;245:103–9.
[9] Inglese M, Park SJ, Johnson G, Babb JS, Miles L, Jaggi H, et al. Deep gray matter perfusion in multiple sclerosis: dynamic susceptibility contrast perfusion magnetic resonance imaging at 3 T. Arch Neurol 2007;64:196–202.
[10] Law M, Saindane AM, Ge Y, Babb JS, Johnson G, Mannon LJ, et al. Microvascular abnormality in relapsing-remitting multiple sclerosis: perfusion MR imaging findings in normal-appearing white matter. Radiology 2004;231:645–52.
[11] Lycke J, Wikkelsö C, Bergh AC, Jacobsson L, Andersen O. Regional cerebral blood flow in multiple sclerosis measured by single photon emission tomography with technetium-99 m hexamethylpropyleneamine oxime. Eur Neurol 1993;33:163–7.
[12] Papadaki EZ, Mastorodemos VC, Amanakis EZ, Tsekouras KC, Papadakis AE, Tsavalas ND, et al. White matter and deep gray matter hemodynamic changes in multiple sclerosis patients with clinically isolated syndrome. Magn Reson Med 2012;68:1932–42.
[13] Paulesu E, Perani D, Fazio F, Comi G, Pozzilli C, Martinelli V, et al. Functional basis of memory impairment in multiple sclerosis: a [18 F]FDG PET study. Neuroimage 1996;4:87–96.
[14] Rashid W, Parkes LM, Ingle GT, Chard DT, Toosy AT, Altmann DR, et al. Abnormalities of cerebral perfusion in multiple sclerosis. J Neurol Neurosurg Psychiatry 2004;75:1288–93.

Please cite this article as: Ota M, et al, Abnormalities of cerebral blood flow in multiple sclerosis: A pseudocontinuous arterial spin labeling MRI study, Magn Reson Imaging (2013), http://dx.doi.org/10.1016/j.mri.2013.03.016

[15] Saindane AM, Law M, Ge Y, Johnson G, Babb JS, Grossman RI. Correlation of diffusion tensor and dynamic perfusion MR imaging metrics in normal-appearing corpus callosum: support for primary hypoperfusion in multiple sclerosis. AJNR Am J Neuroradiol 2007;28:767–72.
[16] Varga AW, Johnson G, Babb JS, Herbert J, Grossman RI, Inglese M. White matter hemodynamic abnormalities precede sub-cortical gray matter changes in multiple sclerosis. J Neurol Sci 2009;282:28–33.
[17] Aslan S, Xu F, Wang PL, Uh J, Yezhuvath US, van Osch M, et al. Estimation of labeling efficiency in pseudocontinuous arterial spin labeling. Magn Reson Med 2010;63:765–71.
[18] Wolff SD, Balaban RS. Magnetization transfer contrast (MTC) and tissue water proton relaxation in vivo. Magn Reson Med 1989;10:135–44.
[19] Detre JA, Alsop DC. Perfusion magnetic resonance imaging with continuous arterial spin labeling: methods and clinical applications in the central nervous system. Eur J Radiol 1999;30:115–24.
[20] Dai W, Garcia D, de Bazelaire C, Alsop DC. Continuous flow-driven inversion for arterial spin labeling using pulsed radio frequency and gradient fields. Magn Reson Med 2008;60:1488–97.
[21] Wong EC. Vessel-encoded arterial spin-labeling using pseudocontinuous tagging. Magn Reson Med 2007;58:1086–91.
[22] Wu WC, Fernandez-Seara M, Detre JA, Wehrli FW, Wang J. A theoretical and experimental investigation of the tagging efficiency of pseudocontinuous arterial spin labeling. Magn Reson Med 2007;58:1020–7.
[23] Polman CH, Reingold SC, Banwell B, Clanet M, Cohen JA, Filippi M, et al. Diagnostic criteria for multiple sclerosis: 2010 revisions to the McDonald criteria. Ann Neurol 2011;69:292–302.
[24] Kurtzke JF. Rating neurologic impairment in multiple sclerosis: an expanded disability status scale (EDSS). Neurology 1983;33:1444–52.
[25] Wang Z, Aguirre GK, Rao H, Wang J, Fernández-Seara MA, Childress AR, et al. Empirical optimization of ASL data analysis using an ASL data processing toolbox: ASLtbx. Magn Reson Imaging 2008;26:261–9.
[26] Cavuşoğlu M, Pfeuffer J, Uğurbil K, Uludağ K. Comparison of pulsed arterial spin labeling encoding schemes and absolute perfusion quantification. Magn Reson Imaging 2009;27:1039–45.
[27] Lu H, Clingman C, Golay X, van Zijl PC. Determining the longitudinal relaxation time (T1) of blood at 3.0 tesla. Magn Reson Med 2004;52:679–82.
[28] Wang J, Zhang Y, Wolf RL, Roc AC, Alsop DC, Detre JA. Amplitude-modulated continuous arterial spin-labeling 3.0-T perfusion MR imaging with a single coil: feasibility study. Radiology 2005;235:218–28.
[29] Pernet C, Andersson J, Paulesu E, Demonet JF. When all hypotheses are right: a multifocal account of dyslexia. Hum Brain Mapp 2009;30:2278–92.
[30] Carter CS, Heckers S, Nichols T, Pine DS, Strother S. Optimizing the design and analysis of clinical functional magnetic resonance imaging research studies. Biol Psychiatry 2008;64:842–9.
[31] Amann M, Achtnichts L, Hirsch JG, Naegelin Y, Gregori J, Weier K, et al. 3D GRASE arterial spin labelling reveals an inverse correlation of cortical perfusion with the white matter lesion volume in MS. Mult Scler 2012;18:1570–6.
[32] Fischer JS, Rudick RA, Cutter GR, Reingold SC. The Multiple Sclerosis Functional Composite Measure (MSFC): an integrated approach to MS clinical outcome assessment. National MS Society Clinical Outcomes Assessment Task Force. Mult Scler 1999;5:244–50.
[33] Riccitelli G, Rocca MA, Pagani E, Martinelli V, Radaelli M, Falini A, et al. Mapping regional grey and white matter atrophy in relapsing-remitting multiple sclerosis. Mult Scler 2012;18:1027–37.
[34] Cifelli A, Arridge M, Jezzard P, Esiri MM, Palace J, Matthews PM. Thalamic neurodegeneration in multiple sclerosis. Ann Neurol 2002;52:650–3.
[35] Behrens TE, Johansen-Berg H, Woolrich MW, Smith SM, Wheeler-Kingshott CA, Boulby PA, et al. Noninvasive mapping of connections between human thalamus and cortex using diffusion imaging. Nat Neurosci 2003;6:750–7.
[36] Buffon F, Molko N, Hervé D, Porcher R, Denghien I, Pappata S, et al. Longitudinal diffusion changes in cerebral hemispheres after MCA infarcts. J Cereb Blood Flow Metab 2005;25:641–50.

Please cite this article as: Ota M, et al, Abnormalities of cerebral blood flow in multiple sclerosis: A pseudocontinuous arterial spin labeling MRI study, Magn Reson Imaging (2013), http://dx.doi.org/10.1016/j.mri.2013.03.016